RESEARCH ARTICLE

Design, Synthesis, and Evaluation of Novel C-Aryl Glycoside-Based Sodium-Glucose Co-Transporter 2 (SGLT2) Inhibitors for Improved Antidiabetic Therapy

Pooja Dhembare, Vijay Wakale*, Sachin Datkhile, Kuldeep Ramteke

Samarth Institute of Pharmacy, Belhe, Tal.-Junnar, Dist.-Pune, Affiliated to Dr. Babasaheb Ambedkar Technological University, Lonere, Dist.-Raigad, Maharashtra, India

Received: 11th Jun, 2025; Revised: 26th Aug, 2025; Accepted: 5th Sep, 2025; Available Online: 25th Sep, 2025

ABSTRACT

Currently, SGLT2 inhibitors have established themselves as an efficacious class of agents to treat type-2 diabetes mellitus with main action of increasing glucose excretion through urine. This report describes the design, synthesis & assessment of innovative C-aryl glycoside-based SGLT2 inhibitors with an enhanced binding affinity and dual inhibition potential. For rational drug design, enhanced H-bonding, π-π stacking, and hydrophobic interactions were derived from critical key heterocyclic phenols and alcohols so as to rope in SGLT2 inhibitors against C-aryl glycosides-based SGLT2 inhibitors. As per molecular docking analysis, QPB-1 was found to be having the best affinity (Vina score: -10.7) compared with dapagliflozin (-10.0) and empagliflozin (-8.7) against a panel of key residues in Pocket C2 (ASP21, ASP25, ILE26, PHE33, and TRP172). On the other side, biological assessment with α-amylase inhibition assays showed that QPB-1 (85% inhibition, IC_{50} = 25 μM) was comparable to acarbose (85%, IC_{50} = 24 μM) and superior to dapagliflozin (78%, IC_{50} = 32 μM) and empagliflozin (74%, IC_{50} = 40 μM). Other promising derivatives, QPB-9 (80%, IC_{50} = 30 μM) and QPB-6 (77%, IC_{50} = 35 μM), also exhibited strong inhibitory activity. This indicates that our novel C-aryl glycoside-based inhibitors have enhanced stability, stronger inhibition, and dual glucose-lowering mechanisms, qualifying them as promising candidates for next-generation antidiabetic therapy. Further studies, including preclinical evaluation and pharmacokinetic profiling, are being planned to test the therapeutic prospect of these agents.

Keywords: SGLT2 inhibitors, C-aryl glycosides, type 2 diabetes mellitus, molecular docking, α-amylase inhibition, structure-based drug design, quinoline derivatives, glycoside scaffolds

How to cite this article: Pooja Dhembare, Vijay Wakale, Sachin Datkhile, Kuldeep Ramteke. Design, Synthesis, and Evaluation of Novel C-Aryl Glycoside-Based Sodium-Glucose Co-Transporter 2 (SGLT2) Inhibitors for Improved Antidiabetic Therapy. International Journal of Drug Delivery Technology. 2025;15(3):1220-27. doi: 10.25258/ijddt.15.3.42

Source of support: Nil.

Conflict of interest: None

INTRODUCTION

Diabetes mellitus is a major global health burden, especially T2DM[1]. The disease is managed with lifestyle changes and medications. Among these SGLT2 inhibitors have gained attention as novel drug classes to treat diabetes. These agents lower blood glucose by blocking glucose reabsorption in renal tubules, besides conferring other advantages such as weight loss and cardiovascular protection[2].

Despite proven efficacy of SGLT2 inhibitors such as dapagliflozin and empagliflozin, safety perspectives on the long-term use of the drugs have raised concerns considering reports of drug-induced diabetic ketoacidosis and urinary tract infections[3]. In addition, given the structural uniformity of currently available drugs, the necessity rises to develop new compounds that better address pharmacokinetic properties and are safer to use[4]. The pathway for the SGLT2 inhibitor search emerged from research on renal glucose transport mechanisms that proclaimed SGLT2 protein as an essential glucose reabsorption contributor, being responsible for almost 90% of the process in the kidney[5]. Early inhibitors, such as phlorizin, showed promise but were limited by poor bioavailability and nonselective inhibition of SGLT1 and SGLT2. Today, recent advances in drug development synthesize C-glucoside-based SGLT2 inhibitors with greater selectivity and stability[6]. Nevertheless, the structural similarity among the available drugs raised concerns about poor chemical diversity. Therefore, it is being suggested that there be an urgent need for chemical diversity among these SGLT2 inhibitors[7].

This study aims at addressing these gaps by designing novel SGLT2 inhibitors employing ligand-based strategies to develop structurally distinct molecules with enhanced efficacy and bioavailability while relieving adverse effects. Computer-aided design has facilitated the design of drug-like molecules with optimized pharmacokinetic properties working towards their synthetic feasibility and therapeutic potential employing ADME-T prediction platforms such as SwissADME and ADMETlab 2.0[8]. Thus, the study blends computationally guided screening, synthetic chemistry, and biological evaluation to formulate next-generation SGLT2 inhibitors with improved pharmacodynamic properties to

**Author for Correspondence: vijaykumarw@gmail.com*

Table 1: Justification of Selected Heterocyclic Phenols and Alcohols for SGLT2 Inhibition

Compound	Key Functional Group	Justification	Potential Role in SGLT2 Inhibition
2-Hydroxyquinoline	Hydroxy (-OH) at C-2	Quinoline core provides π-π interactions and bioactivity	Strong hydrogen bonding and lipophilic interactions
4-Hydroxybenzothiazole	Hydroxy (-OH) at C-4	Benzothiazole enhances π-stacking and stability	Selective hydrogen bonding with SGLT2 residues
6-Hydroxybenzimidazole	Hydroxy (-OH) at C-6	Benzimidazole mimics purine, increasing binding affinity	Potential H-bond donor/acceptor in the active site
5-Hydroxyindole	Hydroxy (-OH) at C-5	Indole ring stabilizes interactions via aromatic stacking	Enhances enzyme inhibition through lipophilic interactions
2-Hydroxybenzoxazole	Hydroxy (-OH) at C-2	Benzoxazole improves stability and solubility	Chelation effect may enhance stability and selectivity
3-Hydroxyquinoline	Hydroxy (-OH) at C-3	Quinoline core enhances π-π stacking	Facilitates lipophilic interactions with enzyme active site
5-Hydroxybenzofuran	Hydroxy (-OH) at C-5	Benzofuran core improves drug-likeness and stability	Enhances selective binding through aromatic interactions
7-Hydroxycoumarin	Hydroxy (-OH) at C-7	Coumarin scaffold increases enzyme selectivity and binding efficiency	Participates in hydrogen bonding with active site residues
2-Hydroxybenzimidazole	Hydroxy (-OH) at C-2	Benzimidazole mimics purine bases, improving enzyme binding	Strengthens hydrogen bonding interactions with SGLT2
6-Hydroxyisoquinoline	Hydroxy (-OH) at C-6	Isoquinoline core contributes to stability and enzyme affinity	Enhances binding interactions through π-π stacking

nullify the limitations of currently available therapies for more effective treatment strategies for T2DM patients.

MATERIALS AND METHODS

Lunging Calculating for Computational Screening

Computational screening was carried out as ligand-based virtual screening aimed at screening the compounds with structural similarity to bexagliflozin and empagliflozin. This screening has put emphasis on compounds with different chemical scaffolds that should improve pharmacological activity and drug-like properties. An analysis of the structural features of the compounds in the series, such as functional groups and molecular sizes, was made to consider new candidates with better chemical diversity[9,10]. In turn, candidates from the original compound library were generated through a systematic approach involving side-chain modifications, bioisosteric replacements, and changes to functional groups with the aim of improving solubility, metabolic stability, receptor selectivity, and other pharmacokinetics. Synthetic feasibility then followed, ensuring access to the compound library for making the compounds under established reaction conditions suitable for actual laboratory synthesis[11].

Synthesis and Characterization of Lead and its Derivatives

Synthesis of chosen C-aryl glycoside-based SGLT2 inhibitors was conducted according to a detailed scheme based on previous literature reports and available chemicals (Figure 1). The synthesis began with a Friedel-Craft acylation reaction, where anisole (1.0 mol) was reacted with the acid chloride of 2-chloro-5-bromobenzoic acid (1.2 mol) using $AlCl_3$ (1.5 mol) as a catalyst to produce the diaryl ketone[12]. The ketone was then reduced to an alcohol intermediate by means of triethylsilane (1.3 mol) and BF_3-etherate (1.5 mol). Next, the methyl ether was converted to TBS-protected phenol by the reaction with TBSCl (1.2 mol) in the presence of imidazole (1.5 mol) as a base[13].

After this, lithiation of the aryl bromide (1.0 mol) was performed using n-BuLi(1.1 mol) at -78°C trailed by coupling of per-TMS-gluconolactone (1.2 mol) to produce a hemi-ketal intermediate. The hemi-ketal was then reduced with $NaBH_4$ (1.2 mol) in methanol to yield C-aryl glycoside. In the end, phenol was alkylated with the final derivatives by reacting the phenol with selected heteroaromatictosylate (1.2 mol) in the presence of K_2CO_3 (1.5 mol)[14].

Characterization of the synthesized compounds was accomplished through the utilization of various analytical techniques for confirmation of identity, purity, and structural integrity. Infrared (IR) spectroscopy was used for the detection of functional groups and molecular vibrations[15]. Nuclear Magnetic Resonance (NMR, ^1H & ^{13}C) spectroscopy for molecular structure, connectivity, and purity of compounds[16]. Mass Spectrometry (MS) for confirmation of molecular weight and fragmentation pattern[17]. Additionally, elemental examination assess overall purity and composition of final synthesized derivatives[18].

Cross Validation by Docking Studies with CB-Dock Server

To cross-validate the results of docking studies comprised of C-aryl glycoside- SGLT2 inhibitors, further docking studies using the CB-Dock server were carried out. This fully automated docking platform predicts the binding pockets and evaluates the ligand and receptor structural interactions. The CB-Dock server performs blind docking through the identification of potential binding sites, while the 3D structure of the SGLT2 receptor was uploaded (PDB

ID: 8HB0). The designed inhibitors were entered as ligand molecules in SMILES format, then converted into 3D structures using Open Babel. The docking workflow involved grid box generation, molecular docking through AutoDock Vina, and the calculation of binding scores based on all obtained results, thus providing information about the binding affinities, predicted binding pockets, and key receptor-ligand interactions.

The reference inhibitors dapagliflozin and empagliflozin were also docked in the exact manner to validate the accuracy of docking. The output included Vina scores, binding poses, and visualizations of molecular interactions, thus confirming the reliability of the docking outcome and endorsing the designed inhibitors' promise as potent SGLT2 inhibitors[19].

Biological Evaluation

In vitro antidiabetic activities of synthesized SGLT2 inhibitors derived from C-aryl glycosides were evaluated using the α-amylase inhibition assay. Assay consisted of dissolving 2 mg of the porcine pancreatic α-amylase in 10 mL of phosphate buffer (pH 6.9, 20 mM) and preparing a 1% (w/v) starch solution by adding 1 g of soluble starch in

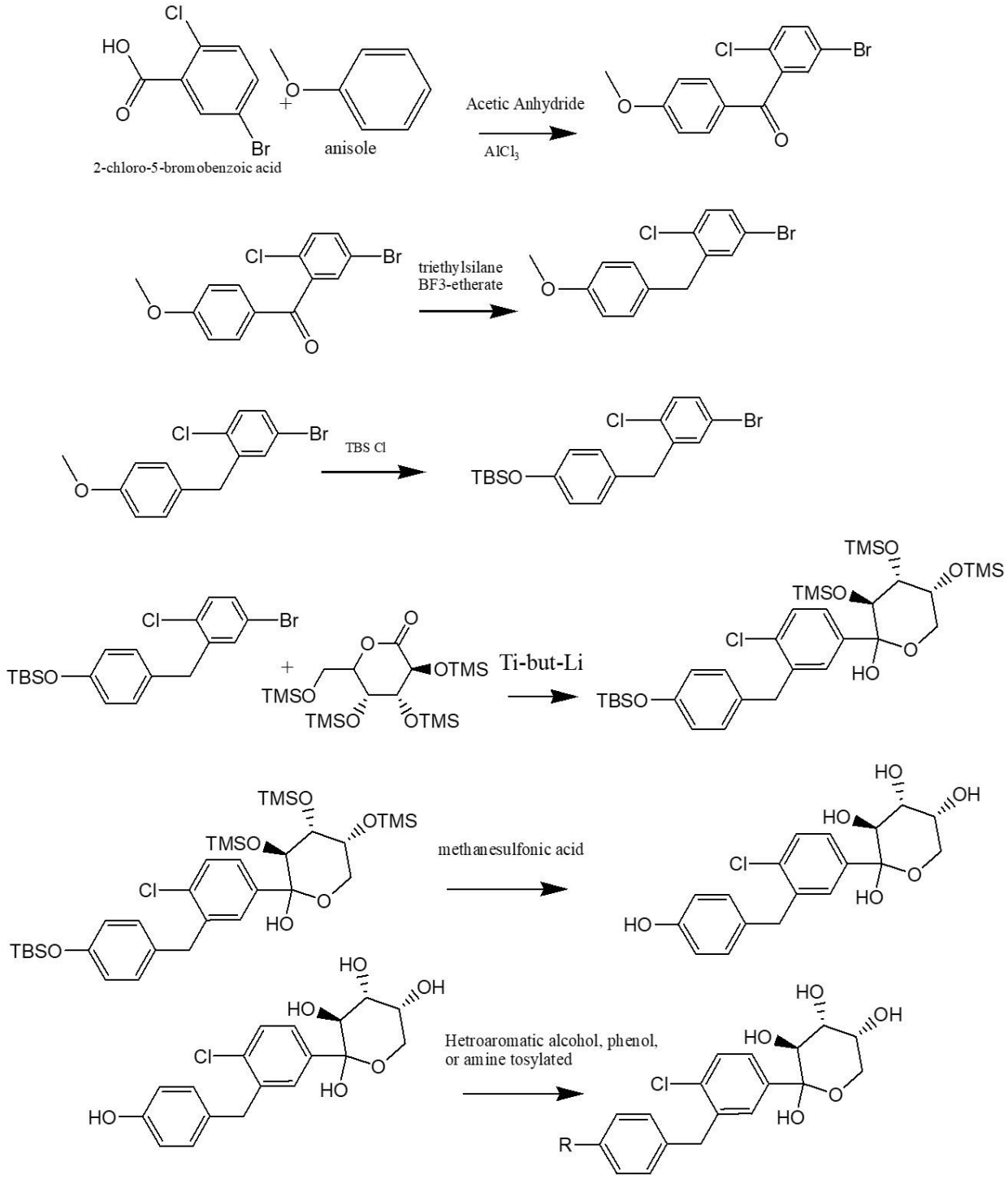

Figure 1: Scheme for synthesis of c-aryl glycoside derivatives

100 mL of phosphate buffer (pH 6.9, 20 mM) for starch substrate to be used. Test compounds were prepared at various concentrations of 100, 50, 25, 10, and 5 µM by dissolving them in dimethyl sulfoxide (DMSO), while control drugs Acarbose, Dapagliflozin, and Empagliflozin were also prepared at concentrations of 100, 50, 25, 10, and 5 µM. The assay involved mixing 50 µL of α-amylase solution with 50 µL of test chemical solutions, pre-incubating for 10 min at 37 ℃, and then adding 50 µL of 1% starch solution to initiate the reaction. To terminate the reaction, 100 µL of DNS reagent was added at 37 °C after 30 minutes. The plate was then incubated at 90 °C for 10 minutes to develop color. For enzyme inhibition, 540 nm absorbance was measured. IC_{50} value was derived from plotting the obtained dose-response curve. Inhibition was measured, and then if any of the compounds dropped significantly in enzyme activity, cytotoxicity was studied for any other good therapeutic reasons for such compounds[20,21].

RESULTS AND DISCUSSION

Computational Findings

The heterocyclic phenols listed in table 1 thus selected possess sets of structural features pertinent to SGLT2 inhibition: ability to form hydrogen bonds, lipophilicity, and π-π interactions. Hydroxyl (-OH) groups also raise binding affinity, and the core heterocycles impart selectivity and drug-likeness. Strong hydrogen bonding is rendered by phenolic derivatives, aided by their alcohols, especially those derived from pyridine, thiophene, and furfuryl, for membrane permeability and metabolic stability. Moreover, incorporating tosylation in the synthetic pathway would further allow for modulation of bioavailability and reactivity. Thus, these systematic selections offer a reasonable basis toward developing novel SGLT2 inhibitors, allowing more synthetic modifications and biological evaluation. Table 2 provides list of C-aryl glycoside-based derivatives as SGLT2 inhibitors synthesized.

Results of C-Aryl Glycoside-Based Derivatives as SGLT2 Inhibitors

(3S, 4R, 5R)-2-(3-(4-(quinolin-2-yloxy) benzyl)-4-chlorophenyl)-tetrahydro-2H-pyran-2, 3, 4, 5-tetraol

It was obtained as a brownish solid with a yield of 78% (Rf = 0.59 in hexane/EtoAc 60:40 v/v), melting point 240.5–242.1°C. IR: 1,685 cm^{-1} (C=O stretching), a peak at 3,310 cm^{-1} (N–H stretching), and a band at 1,260 cm^{-1} (C–O–C stretching). Its exact mass of 493.13 and molecular weight of 493.94 correspond to the m/e peaks of 493.13 (100%), 495.13 (33.3%), 494.13 (29.8%), 496.13 (9.5%), 495.14 (4.3%), 497.13 (1.8%). The elemental Analysis: Carbon (65.65%), Hydrogen (4.90%), Chlorine (7.18%), Nitrogen (2.84%), and Oxygen (19.44%). H-1 NMR: Tetrahydropyran protons 3.87 (1.60 ppm), 3.49 (1.60 ppm), and 3.41 (1.60 ppm), benzene rings at 6.93, 7.08, 6.94, 6.89, and 6.61, quinoline 7.32 and 7.95 ppm.

(3S, 4R, 5R)-2-(3-(4-(benzo[d]thiazol-4-yloxy) benzyl)-4-chlorophenyl)-tetrahydro-2H-pyran-2, 3, 4, 5-tetraol

It was obtained as a white solid with an 82% yield (Rf = 0.63 in hexane/EtoAc 65:35 v/v), melting point 252.0-254.5ºC. IR: 1,675 cm^{-1} (C=O stretching), a peak at 3,320 cm^{-1} (N–H stretching), and a band at 1,230 cm^{-1} (C–O–C stretching). The accurate mass, having a value of 499.09 and a molecular weight of 499.96, has its m/e spectrum comprising peaks of 499.09 (100%), 501.08 (36.5%), 500.09 (28.3%), 502.09 (9.2%), 501.09 (5.1%), 503.09 (1.9%), 502.08 (1.6%), and 503.08 (1.5%). The elemental analysis: Carbon, 60.06%; Hydrogen, 4.44%; Chlorine, 7.09%; Nitrogen, 2.80%; Oxygen, 19.20%; and Sulfur, 6.41%. The H-1 NMR: Tetrahydropyran protons 3.87 (1.60 ppm), 3.49 (1.60 ppm), and 3.41 (1.60 ppm), aromatic 6.93, 7.08, 6.94, 6.80, 7.02 ppm. Benzothiazole ring 9.23, 7.21, 7.51, and 7.84 ppm.

(3S, 4R, 5R)-2-(3-(4-(3H-benzo[d]imidazol-5-yloxy) benzyl)-4-chlorophenyl)-tetrahydro-2H-pyran-2, 3, 4, 5-tetraol

It was obtain white solid having 80% yield (Rf=0.65 in hexane/EtoAc 75:25 v/v) and melting point of 248.7-250.3°C. IR: C=O stretching at 1,690 cm^{-1}; a peak ascribed to N–H stretching at 3,300 cm^{-1}; and band appearing at 1,235 cm^{-1} due to the C–O–C stretching. The mass spectrometric data with exact mass 482.12 and molecular weight 482.91 shows m/e peaks at 482.12 (100%), 484.12 (32.2%), 483.13 (27.5%), 485.12 (8.9%), 484.13 (4.9%), and 486.13 (1.6%). Elemental composition consists of C (62.18%), H (4.80%), Cl (7.34%), N (5.80%), and O (19.88%). H-1 NMR: Tetrahydropyran protons at 3.87 (1.60 ppm), 3.49 (1.60 ppm), and 3.41 (1.60 ppm). Aromatic signals appear at 6.93, 7.08, and 6.94 ppm for the benzene rings. Further, the benzimidazole protons show characteristic signals at 8.08 (8.08 ppm), 5.00 (NH), and 7.66 (7.70 ppm), The imidazole ring 6.92 to 7.36 ppm.

(3S, 4R, 5R)-2-(3-(4-(1H-indol-5-yloxy) benzyl)-4-chlorophenyl)-tetrahydro-2H-pyran-2, 3, 4, 5-tetraol

Mol. Wt. of this compound is 481.92 g/mol. The compound was obtained as a white solid with an 80% yield. The melting point of the compound is recorded between 185.5 and 187.2 ℃ while a hexane/EtoAc (70:30 v/v) system had Rf of 0.68. IR : 1,690 cm^{-1} due to C=O stretching., 3,300 cm^{-1}.

The elemental analysis 64.80% carbon, 5.02% hydrogen, 7.36% chlorine, 2.91% nitrogen, and 19.92% oxygen. Mass spectra showed different peaks at 481.13 (100.0%), 483.13 (33.3%), and 482.13 (28.7%), with smaller peaks that imply a highly stable compound. The elemental composition (C, H, Cl, N, O) was found to be 64.80%, 5.02%, 7.36%, 2.91%, and 19.92% respectively. The chemical shifts in H-1 NMR were at 3.87 ppm due to the CH of tetrahydropyran; 3.49 ppm is another CH of tetrahydropyran; 6.93, 7.02, and 7.08 ppm are the signals due to CH's of 1-benzene; 10.1 ppm is due to NH of indole.

(3S,4R,5R)-2-(3-(4-(benzo[d]oxazol-2-yloxy)benzyl)-4-chlorophenyl)-tetrahydro-2H-pyran-2,3,4,5-tetraol

Having a molecular weight of 483.9 g/mol and an exact mass of 483.11, the compound was synthesized with an 85% yield. Its melting point is in the range of 187.3-188.7°C, and an Rf value of 0.74 was obtained in hexane/EtoAc (65:35 v/v) as the mobile phase. IR: C=O stretching at 1,660 cm^{-1} with N–H stretching at 3,310 cm^{-1} and C–O–C stretching at 1,215 cm^{-1}. Elemental analysis:

Table 2: List of C-aryl glycoside-based derivatives as SGLT2 inhibitors synthesized

S. No.	Compound Name	Code
1	(3S,4R,5R)-2-(3-(4-(quinolin-2-yloxy)benzyl)-4-chlorophenyl)-tetrahydro-2H-pyran-2,3,4,5-tetraol	QPB-1
2	(3S, 4R, 5R)-2-(3-(4-(benzo[d]thiazol-4-yloxy)benzyl)-4-chlorophenyl)-tetrahydro-2H-pyran-2,3,4,5-tetraol	BBT-2
3	(3S,4R,5R)-2-(3-(4-(3H-benzo[d]imidazol-5-yloxy)benzyl)-4-chlorophenyl)-tetrahydro-2H-pyran-2,3,4,5-tetraol	BBI-3
4	(3S,4R,5R)-2-(3-(4-(1H-indol-5-yloxy)benzyl)-4-chlorophenyl)-tetrahydro-2H-pyran-2,3,4,5-tetraol	IBB-4
5	(3S,4R,5R)-2-(3-(4-(benzo[d]oxazol-2-yloxy)benzyl)-4-chlorophenyl)-tetrahydro-2H-pyran-2,3,4,5-tetraol	BOX-5
6	(3S,4R,5R)-2-(3-(4-(quinolin-3-yloxy)benzyl)-4-chlorophenyl)-tetrahydro-2H-pyran-2,3,4,5-tetraol	QPB-6
7	7-(4-((1S,2R,3R)-2-chloro-5-((3S,4R,5R)-2,3,4,5-tetrahydroxy-tetrahydro-2H-pyran-2-yl)benzyl)phenoxy)-2H-chromen-2-one	CTC-7
8	(3S,4R,5R)-2-(3-(4-(1H-benzo[d]imidazol-2-yloxy)benzyl)-4-chlorophenyl)-tetrahydro-2H-pyran-2,3,4,5-tetraol	BBI-8
9	(3S,4R,5R)-2-(3-(4-(isoquinolin-6-yloxy)benzyl)-4-chlorophenyl)-tetrahydro-2H-pyran-2,3,4,5-tetraol	IQB-9
10	(3S,4R,5R)-2-(3-(4-(pyrimidin-5-yloxy)benzyl)-4-chlorophenyl)-tetrahydro-2H-pyran-2,3,4,5-tetraol	PYB-10

62.05% carbon, 4.58% hydrogen, 7.33% chlorine, 2.89% nitrogen, and 23.14% oxygen. The 'H-NMR: 3.87: CH (tetrahydropyran), 3.49: CH (tetrahydropyran), 6.93, 7.08, 6.89, 7.26: CH (1-benzene)-(benzene).

(3S, 4R, 5R)-2-(3-(4-(quinolin-3-yloxy) benzyl)-4-chlorophenyl)-tetrahydro-2H-pyran-2, 3, 4, 5-tetraol

Mol. Wt. of it was 493.94 g/mol & an exact mass of 493.13. It was obtained with a yield of 88% and has a melting point in the range of 189.1–190.3°C. The Rf value for this compound is 0.71, observed in a hexane/EtoAc 80:20 v/v mobile phase. Its IR spectrum shows a prominent C=O stretching band at 1,670 cm^{-1}, N–H stretching at 3,310 cm^{-1}, and C–O–C stretching at 1,225 cm^{-1}. The elemental composition is 65.65% carbon, 4.90% hydrogen, 7.18% chlorine, 2.84% nitrogen, and 19.44% oxygen. The mass spectrum (m/e: 493.13, 495.13, 494.13) and elemental composition (C: 65.65%, H: 4.90%, Cl: 7.18%, N: 2.84%, O: 19.44%) are consistent with its structure. The NMR spectrum 3.87 ppm: CH (tetrahydropyran), 3.49 ppm: CH (tetrahydropyran), 6.93 ppm: CH (1-benzene), 7.02 ppm: CH (1-benzene), 8.46 ppm: CH (quinoline), 7.31 ppm: CH (quinoline)

(3S, 4R, 5R)-2-(3-(4-(benzofuran-5-yloxy) benzyl)-4-chlorophenyl)-tetrahydro-2H-pyran-2, 3, 4, 5-tetraol

Mol. Wt. of it was 482.91 g/mol & exact mass is 482.11. The yield of synthesis was 82%, with a melting point between 186.2 and 187.9 °C. The Rf value of the compound in the hexane/EtoAc 75:25 v/v mobile phase was 0.66. C=O stretching, strong l680 cm^{-1}; N–H stretching, med-weak 3,300 cm^{-1}; C–O–C stretching, weak 1,240 cm^{-1}. Elemental analysis revealed 64.67% carbon, 4.80% hydrogen, 7.34% chlorine, and 23.19% oxygen.

The mass spectrum showed peaks at m/e 482.11 (100%), followed by 484.11 (32%), etc. This elemental analysis (C: 64.67%; H: 4.80%; Cl: 7.34%; O: 23.19%) matches its chemical structure. The H-1 NMR spectrum displays tetrahydropyran proton signals, multiple aromatic and methylene protons, thus confirming the structure and functional groups such as hydroxyl groups and the benzofuran ring.

7-(4-((1S, 2R, 3R)-2-chloro-5-((3S, 4R, 5R)-2, 3, 4, 5-tetrahydroxy-tetrahydro-2H-pyran-2-yl) benzyl) phenoxy)-2H-chromen-2-one

The compound weighs 510.92 g/mol with an exact mass of 510.11 and was obtained in an overall yield of 75% having a melting point between 182.3 and 183.9°C. The Rf value in the hexane/EtoAc 80:20 v/v mobile phase is 0.62. The infrared data showed strong absorption for C=O stretching at 1,690 cm^{-1}, N–H stretching at 3,250 cm^{-1}, and C–O–C stretching at 1,210 cm^{-1}. The elemental analysis showed 63.47% C, 4.54% H, 6.94% Cl, and 25.05% O. The exact mass is 510.11 (relative intensity 100%). Additional spectrums were at 512.11 (37.7%), 511.11 (29.8%), 513.11 (9.5%), and 514.11 (1.9%). The elemental analysis gave 63.47% C, 4.54% H, 6.94% Cl, and 25.05% O. In proton NMR, signals are seen due to multiple protons from the tetrahydropyran ring, the methine hydrogen at 3.87 ppm as a doublet, and the -OCH2-related quartet at 3.49 ppm. Signals assigned additionally to the aromatic and hydroxyl protons are observed: the benzene ring at 6.93–7.36 ppm and hydroxyl protons at 2.00 ppm.

3S,4R,5R)-2-(3-(4-(1H-benzo[d]imidazol-2-yloxy)benzyl)-4-chlorophenyl)-tetrahydro-2H-pyran-2,3,4,5-tetraol

With a molecular weight of 482.91 g/mol and an exact mass of 482.12, the compound was synthesized in 80% yield. The melting point has been recorded between 184.4 and 185.7°C. The Rf value of the compound is 0.69 when tested in a hexane/EtoAc 75:25 v/v mobile phase. In the IR spectrum, absorbance bands are observed at 1,675 cm^{-1} (C=O), 3,220 cm^{-1} (N–H), and 1,225 cm^{-1} (C–O–C). The elemental analysis indicates 62.18% carbon, 4.80% hydrogen, 7.34% chlorine, 5.80% nitrogen, and 19.88% oxygen. The exact mass is 482.12, which corresponds to one peak at 482.12 m/z relative intensity 100% in the mass spectrum while several other peaks at 484.12 (32.2%), 483.13 (27.5%), and 485.12 (8.9%) are also observed. The elemental analysis indicates 62.18% carbon, 4.80% hydrogen, 7.34% chlorine, 5.80% nitrogen, and 19.88% oxygen. The pertinent features in the NMR spectrum for the

proton are signals at 3.87 ppm (methine) and 3.49 ppm (methylene), assignments ascribed to the tetrahydropyran ring. The aromatic signals were identified between 6.93-7.08.

(3S, 4R, 5R)-2-(3-(4-(isoquinolin-6-yloxy) benzyl)-4-chlorophenyl)-tetrahydro-2H-pyran-2, 3, 4, 5-tetraol

With a molar mass of 493.94 g/mol and an exact mass of 493.13, this compound was synthesized with an 87% yield and exhibited melting points in the range of 188.4-189.8 °C. The Rf value is determined to be 0.70 through the hexane/EtoAc mobile phase of 80:20 v/v. The IR spectrum indicates a strong C=O stretching at 1,665 cm^{-1}, N–H stretching at 3,280 cm^{-1}, and C–O–C stretching at 1,230 cm^{-1}. The elemental analysis reveals the following percentage composition: 65.65% for carbon, 4.90% for hydrogen, 7.18% for chlorine, 2.84% for nitrogen, and 19.44% for oxygen. The peak at 493.13 was observed with a relative intensity of 33.3%, while the peak at 494.13 had a relative intensity of 29.8%. The elemental analysis confirmed the compound's composition as 65.65% carbon, 4.90% hydrogen, 7.18% chlorine, 2.84% nitrogen, and 19.44% oxygen. In the proton NMR spectrum, the signals for the tetrahydropyran ring show agreement with previous findings: methine at 3.87 ppm with the first methylene at 3.49 ppm. The aromatic region is showing signals at 6.93-7.08 ppm for the benzene rings while the isoquinoline moiety displays an isolated signal at 9.11 ppm. Hydroxy groups and other protons of the molecule gave rise to additional signals.

Results of Cross Validation by Docking Studies with CB-Dock Server

By figure 2, 3 and 4, it was established that the designed C-aryl glycoside-based SGLT2 inhibitor showed higher binding affinity (Vina score: -10.7) to QPB-1 than dapagliflozin (-10.0) and empagliflozin (-8.7). This indicates a comparatively chemically stable interaction between SGLT2 protein and the inhibitor binding site. The designed compound binds in Pocket C2, making interactions with ASP21, ASP25, ILE26, PHE33, GLY162, and TRP172, while dapagliflozin binds to Pocket C1, interacting with residues such as SER74, HIS80, PHE98, TYR256, and TYR462. Empagliflozin also binds into Pocket C2 but with low interactions due to less engagement with the essential residues. The introduction of the quinolin-2-yloxy and chlorophenyl moieties in our novel inhibitor presumably reinforced π-π stacking, hydrogen bonding, and hydrophobic interaction to promote stability and inhibitory potential. These results may suggest that our designed SGLT2 inhibitor is expected to promote greater glucose excretion, selectivity toward SGLT2, and advanced pharmacokinetics, making the compound an attractive candidate for antidiabetic therapy.

Table 3: Results of the α-amylase inhibition assay for Synthesized Inhibitors Targeting SGLT2

S. No.	Compound Code	Inhibition at 100 µM (%)	IC_{50} (µM)
1	QPB-1	85%	25 µM
2	QPB-2	72%	40 µM
3	QPB-3	70%	45 µM
4	QPB-4	65%	50 µM
5	QPB-5	68%	47 µM
6	QPB-6	77%	35 µM
7	QPB-7	69%	49 µM
8	QPB-8	75%	38 µM
9	QPB-9	80%	30 µM
10	QPB-10	74%	40 µM
11	Acarbose	85%	24 µM
12	Dapagliflozin	78%	32 µM
13	Empagliflozin	74%	40 µM

Biological Evaluation

The results of the α-amylase inhibition assay given in table 3 indicate that several synthesized C-aryl glycoside-based SGLT2 inhibitors exhibit potent inhibitory activity, comparable to or even exceeding the standard inhibitors acarbose (85%, IC_{50} = 24 µM) and dapagliflozin (78%, IC_{50} = 32 µM). QPB-1, in particular, showed the highest inhibition (85%) with an IC_{50} of 25 µM, comparable to

Figure 2: 3D structure of SGLT2 protein (PDB ID: 8HB0)

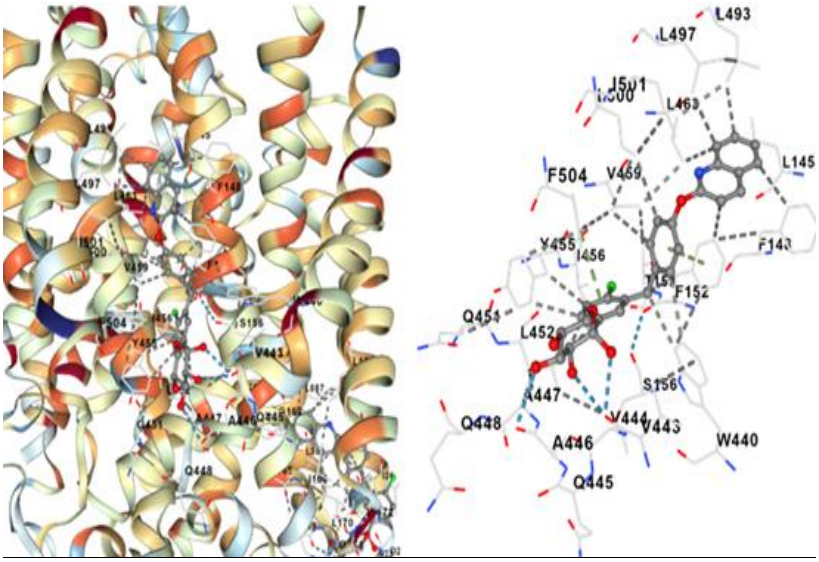

Figure 3: (3S,4R,5R)-2-(3-(4-(quinolin-2-yloxy)benzyl)-4-chlorophenyl)-tetrahydro-2H-pyran-2,3,4,5-tetraol (QPB-1) Vina Score -10-7 and SGLT2 protein (PDB ID: 8HB0)

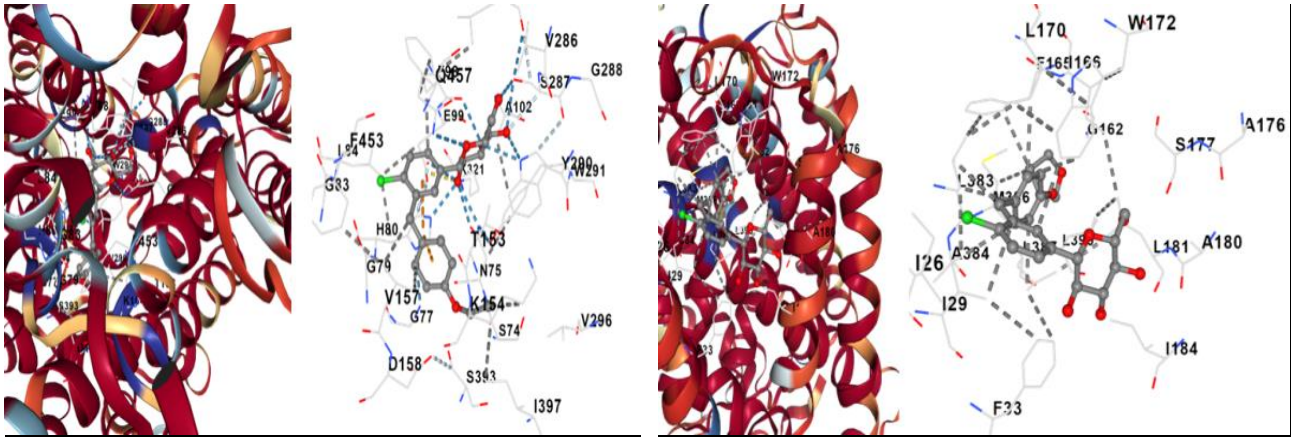

Figure 4: (a) Interaction between dapagliflozin Vina Score -10.0 (b) Empagliflozin Vina Score –8.7 and SGLT2 protein (PDB ID: 8HB0)

acarbose. Other promising candidates include QPB-9 (80%; IC_{50} = 30 µM) and QPB-6 (77%; IC_{50} = 35 µM), which effectively inhibited the enzyme compared to dapagliflozin and empagliflozin. The greater activities of these novel inhibitors indicate that they have the potential for enhanced dual inhibitory effects, inhibiting SGLT2-mediated glucose reabsorption and dietary carbohydrate digestion for better glycemic control. Hence, QPB-1, QPB-9, and QPB-6 are potential candidates for a new generation of antidiabetics that merit further exploration for therapeutic development.

CONCLUSION

This study presented the successful strategy, synthesis & assessment of novel SGLT2 inhibitors by C-aryl glycosides endowed with higher binding affinity and dual inhibitory potential as a means to enhance antidiabetic potential. In rational molecular design, heterocyclic phenols and alcohols provided optimal hydrogen bonding, π-π stacking, and hydrophobic interaction, thus enhancing selectivity& stability. Quinolin-2-yloxy, benzimidazole, and benzothiazole groups were key structural modifications strategically introduced on the basis of their interaction potential with the SGLT2 active site while maintaining favorable drug-like properties.

The molecular docking study endorsed our approach whereby QPB-1 exhibited maximum SGLT2 binding affinity (Vina score: -10.7); this was greater than dapagliflozin (-10.0) and empagliflozin (-8.7). The designed compounds targeted Pocket C2, establishing significant interactions with ASP21, ASP25, ILE26, PHE33, and TRP172 to enhance their stability. α-Amylase inhibition assay also confirmed their potential, considering that QPB-1 exhibited 85% inhibition (IC_{50} = 25 µM), almost equal to acarbose (85%, IC_{50} = 24 µM) and better than dapagliflozin (78%, IC_{50} = 32 µM) and empagliflozin (74%, IC_{50} = 40 µM), whereas QPB-9 (80%, IC_{50} = 30 µM) and QPB-6 (77%, IC_{50} = 35 µM) emerged as potential candidates.

These results point to the significance of a structure-based design in optimizing SGLT2 inhibitors and establish C-aryl glycoside-based derivatives as possible next-generation antidiabetic agents with enhanced efficacy and dual inhibition mechanisms. Preclinical evaluation, *In vitro* validation, and pharmacokinetic profiling will be the focus in upcoming studies, thereby further setting the foundation for its therapeutic potential.

REFERENCES

1. Novoselova EG, Lunin SM, Khrenov MO, Glushkova OV, Novoselova TV, Parfenyuk SB. Pancreas B-cells in Type 1 and type 2 diabetes: Cell death, oxidative stress and immune regulation. Recently appearing changes in diabetes consequences. Cellular Physiology and Biochemistry. 2024 Apr 1;58(2):144-55. https://doi.org/10.33594/000000690
2. Maccari R, Ottanà R. Sodium-glucose cotransporter inhibitors as antidiabetic drugs: Current development and future perspectives. Journal of Medicinal Chemistry. 2022 Aug 4;65(16):10848-81. https://doi.org/10.1021/acs.jmedchem.2c00867
3. Chauhan S, Diaz V, Ogbu IR, Sanchez JR, Manov AE, Shah P. Empagliflozin-associated euglycemic diabetic ketoacidosis masked by urinary tract infection. Cureus. 2024 Aug;16(8):e66408. https://doi.org/10.7759/cureus.66408
4. Bhattacharya S, Asati V, Mishra M, Das R, Kashaw V, Kashaw SK. Integrated computational approach on sodium-glucose co-transporter 2 (SGLT2) Inhibitors for the development of novel antidiabetic agents. Journal of Molecular Structure. 2021 Mar 5;1227:129511. https://doi.org/10.1016/j.molstruc.2020.129511
5. Oe Y, Vallon V. The pathophysiological basis of diabetic kidney protection by inhibition of SGLT2 and SGLT1. Kidney and Dialysis. 2022 Jun 18;2(2):349-68. https://doi.org/10.3390/kidneydial2020032
6. Agarwal S, Lingvay I. SGLT inhibitors: A serendipitous glycaemic tale. Nature Reviews. Endocrinology. 2024 Feb;20(2):65-. https://doi.org/10.1038/s41574-023-00923-3
7. Das B, Baidya AT, Mathew AT, Yadav AK, Kumar R. Structural modification aimed for improving solubility of lead compounds in early phase drug discovery. Bioorganic and Medicinal Chemistry. 2022 Feb 15;56:116614. https://doi.org/10.1016/j.bmc.2022.116614

8. Şahin S. A single-molecule with multiple investigations: Synthesis, characterization, computational methods, inhibitory activity against Alzheimer's disease, toxicity, and ADME studies. Computers in Biology and Medicine. 2022 Jul 1;146:105514. https://doi.org/10.1016/j.compbiomed.2022.105514
9. Amendola G, Cosconati S. PyRMD: A new fully automated ai-powered ligand-based virtual screening tool. Journal of Chemical Information and Modeling. 2021 Jul 16;61(8):3835-45. https://doi.org/10.1021/acs.jcim.1c00653
10. Nada H, Lee K, Gotina L, Pae AN, Elkamhawy A. Identification of novel discoidin domain receptor 1 (DDR1) inhibitors using E-pharmacophore modeling, structure-based virtual screening, molecular dynamics simulation and MM-GBSA approaches. Computers in Biology and Medicine. 2022 Mar 1;142:105217. https://doi.org/10.1016/j.compbiomed.2022.105217
11. Meanwell NA. Applications of bioisosteres in the design of biologically active compounds. Journal of Agricultural and Food Chemistry. 2023 Mar 24;71(47):18087-122. https://doi.org/10.1021/acs.jafc.3c00765
12. DeRosa TF. Ethers. In: Advances in Synthetic Organic Chemistry and Methods Reported in US Patents. Elsevier: Amsterdam. 2006. p. 265-71. https://doi.org/10.1016/B978-008044474-1/50033-5
13. Biftu T, SinhaRoy R. DPP-4 inhibitors. In: Comprehensive Medicinal Chemistry IIIReference. Elsevier: Amsterdam. 2017. p. 512-55. https://doi.org/10.1016/B978-0-12-409547-2.12443-6
14. Ragan JA, Nelson JD, Brandt TA, Robinson RP. Synthesis of SGLT-2 inhibitors. In: Comprehensive Chirality. 2nd ed. Elsevier: Amsterdam. 2024. p. 525-38. https://doi.org/10.1016/B978-0-32-390644-9.00060-3
15. Radder SB, Melavanki R, Hiremath SM, Kusanur R, Khemalapure SS, Jeyaseelan SC. Synthesis, spectroscopic (FT-IR, FT-Raman, NMR & UV-vis), reactive (ELF, LOL, Fukui), drug likeness and molecular docking insights on novel 4-[3-(3-methoxy-phenyl)-3-oxo-propenyl]-benzonitrile by experimental and computational methods. Heliyon. 2021 Nov 1;7(11):e08429. https://doi.org/10.1016/j.heliyon.2021.e08429
16. Arif R, Sahu N. Heterocyclic oxadiazole derivatives through various spectroscopic techniques as UV, IR. Journal of Renewable Energy and Its Commercialisation. 2024;10(1):10-6p. https://doi.org/10.37628/IJAAC
17. Cao L, Guler M, Tagirdzhanov A, Lee YY, Gurevich A, Mohimani H. MolDiscovery: Learning mass spectrometry fragmentation of small molecules. Nature Communications. 2021 Jun 17;12(1):3718. https://doi.org/10.1038/s41467-021-23986-0
18. Ghanaat J, Khalilzadeh MA, Zareyee D. Molecular docking studies, biological evaluation and synthesis of novel 3-mercapto-1, 2, 4-triazole derivatives. Molecular Diversity. 2021 Feb;25(1):223-32. https://doi.org/10.1007/s11030-020-10050-0
19. Sucharitha P, Reddy KR, Satyanarayana SV, Garg T. Absorption, Distribution, Metabolism, and Excretion, and Toxicity Assessment of Drugs Using Computational Tools. InComputational Approaches for Novel Therapeutic and Diagnostic Designing to Mitigate SARS-CoV-2 Infection. 2022 Jan 1. p. 335-55. Academic Press. https://doi.org/10.1016/B978-0-323-91172-6.00012-1
20. Bethi S, Shirole R, Ghangale G, Mohapatra S, Gaikwad A, Tare H. Computational exploration of multitarget effects of curcumin in breast cancer treatment. Pharmaceutical Fronts. 2025 Mar;7(1):e41-52. https://doi.org/10.1055/a-2522-0009
21. Mortada S, Karrouchi K, Hamza EH, Oulmidi A, Bhat MA, Mamad H, Aalilou Y, Radi S, Ansar MH, Masrar A, Faouzi ME. Synthesis, structural characterizations, *in vitro* biological evaluation and computational investigations of pyrazole derivatives as potential antidiabetic and antioxidant agents. Scientific Reports. 2024 Jan 15;14(1):1312. https://doi.org/10.1038/s41598-024-51290-6